REPORT DOCUMENTATION PAGE

Form Approved
OMB No. 0704-0188

1. REPORT DATE *(DD-MM-YYYY)*

2. REPORT DATE
August 1999

3. DATES COVERED *(From - To)*
Final 3/22/96 - 9/22/96

4. TITLE AND SUBTITLE
Optical Processing for Sonar Arrays

5a. CONTRACT NUMBER
N00014-96-C-2045

5b. GRANT NUMBER

5c. PROGRAM ELEMENT NUMBER

5d. PROJECT NUMBER

5e. TASK NUMBER

5f. WORK UNIT NUMBER

6. AUTHOR(S)
Kelvin Wagner, Dana Anderson, Lloyd Griffiths

7. PERFORMING ORGANIZATION NAME(S) AND ADDRESS(ES)
University of Colorado
Optoelectronic Computing Systems Center
Campus Box 525
Boulder, CO 80309-0525

8. PERFORMING ORGANIZATION REPORT NUMBER
1536910

9. SPONSORING/MONITORING AGENCY NAME(S) AND ADDRESS(ES)
Dr. John Lee
Naval Research Laboratory
Washington, DC 20375-5338

10. SPONSOR/MONITOR'S ACRONYM(S)

11. SPONSORING/MONITORING AGENCY REPORT NUMBER

12. DISTRIBUTION AVAILABILITY STATEMENT
Unlimited

19990921 034

13. SUPPLEMENTARY NOTES

14. ABSTRACT
We present an adaptation of the BEAMTAP (Broadband and Efficient Adaptive Method for True-time-delay Array Processing) algorithm, previously developed for wideband phased array radars, to lower bandwidth applications such as sonar. This system utilizes the emerging time or wavelength multiplexed optical hydro-phone sensors and processes the cohered array of signals in the optical domain without conversion to the electronic domain or digitization. Modulated signals from an optical hydro-phone array are pre-processed then imaged through a photorefractive crystal where they interfere with a reference signal and its delayed replicas. The diffraction of the sonar signals off these adaptive weight gratings and detection on a linear time-delay-and-integrate charge coupled device (TDI CCD) completes the true-time-delay (TTD) beamforming process. Optical signals focused on different regions of the TDI CCD accumulate the appropriate delays necessary to synchronize and coherently sum the acoustic signals arriving at various angles on the hydro-phone array. In this report, we present an experimental demonstration of TTD processing of low frequency signals (in the KHz sonar regime) using a TDI CCD tapped delay line. Simulations demonstrating the performance of the overall system are also presented.

15. SUBJECT TERMS
Adaptive array processing, sonar, photorefractive crystals, optical processing

16. SECURITY CLASSIFICATION OF: a. REPORT	b. ABSTRACT	c. THIS PAGE	17. LIMITATION OF ABSTRACT	18. NUMBER OF PAGES	19a. NAME OF RESPONSIBLE PERSON
U	U	U	UL	18	Kelvin Wagner
					19b. TELEPONE NUMBER *(Include area code)* 303-492-4661

Optical Processing for Sonar Arrays

Kelvin Wagner
Dept of ECE
box 425
University of Colorado
Boulder CO 80309-0425
Phone : (303)492-4661
FAX : (303)492-5810
email : kelvin@colorado.edu

Dana Anderson
Dept of Physics
box 440
University of Colorado
Boulder CO 80309-0440

Lloyd Griffiths, Dean
School of Information Technology
100 Science and Technology II, ms 4A3
George Mason University
Fairfax VA 22030-4444

Program Manager: **Dr. John Lee**
code 5623
Naval Research Lab
office b216/200m
4555 Overlook Ave., SW
(202)-767-3100
lee8@ccf.nrl.navy.mil

Period of Performance:	(6 months) Mar 22 1996 – Sept 22 1996
Budget:	$50,000
NRL funding number	N00014-96-C-2045

ABSTRACT

We present an adaptation of the BEAMTAP (Broadband and Efficient Adaptive Method for True-time-delay Array Processing) algorithm, previously developed for wideband phased array radars, to lower bandwidth applications such as sonar. This system utilizes the emerging time or wavelength multiplexed optical hydro-phone sensors and processes the cohered array of signals in the optical domain without conversion to the electronic domain or digitization. Modulated signals from an optical hydro-phone array are pre-processed then imaged through a photorefractive crystal where they interfere with a reference signal and its delayed replicas. The diffraction of

the sonar signals off these adaptive weight gratings and detection on a linear time-delay-and-integrate charge coupled device (TDI CCD) completes the true-time-delay (TTD) beamforming process. Optical signals focused on different regions of the TDI CCD accumulate the appropriate delays necessary to synchronize and coherently sum the acoustic signals arriving at various angles on the hydro-phone array. In this paper, we present an experimental demonstration of TTD processing of low frequency signals (in the KHz sonar regime) using a TDI CCD tapped delay line. Simulations demonstrating the performance of the overall system are also presented.

Keywords: Optical Signal processing, adaptive arrays, true-time-delay, sonar beamforming.

1 Hydro-phone Array Processing

The underwater array sensing, beamforming, imaging, and target classification problem using sea floor fixed, towed, or floating sonobouy hydrophones with arrays of fiber multiplexed optical sensors, as illustrated in Figure 1, is an extremely challenging problem. In this paper, we show how to solve the sonar array processing problem using a novel class of optical processors that requires only 2 tapped-delay-lines which we have previously employed as an adaptive beamformer and jammer nuller for phased array radar signals.[1, 2] Using the massively parallel LMS adaptation of holographically stored adaptive weights results in a processing throughput that can track the real-time adaptive requirements of the hydro-phone array imaging problem.

We present real-time approaches that exploit the optical nature of the data emerging from arrays of optically interrogated hydro-phone sensors[3] to directly allow adaptive multiple beamforming and imaging in a small power-efficient real-time optical processor. The many well known difficulties encountered in both passive and active sonar include multi-path echoes, dispersive

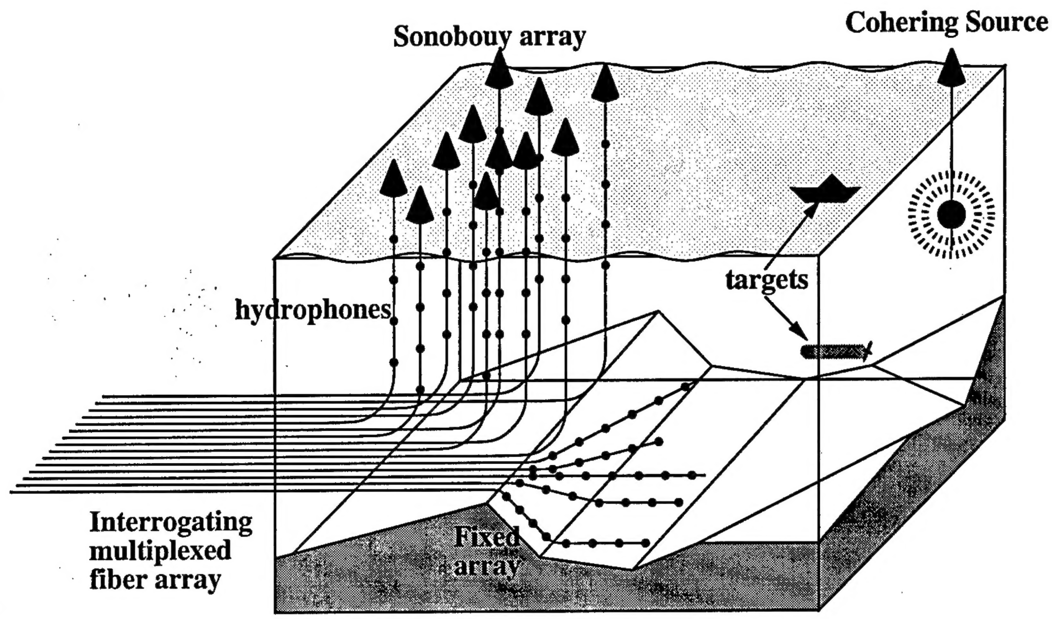

Figure 1: Hydrophones are connected either to a floating buoy or fixed to the sea bed and fiber linked as shown. A single source can be used to provide a reference tone to cohere the array.

media, frequency dependent absorption, inhomogeneities, Doppler shifts, poorly sampled and drifting arrays, hydrophonics and interference. Fully adaptive systems may be able to deal with most if not all of these difficulties, but are usually abandoned due to tremendous computational burdens which are well beyond even the most optimistic projections for massively parallel multi-DSP chip implementations. Consider, for example, an array of $n_1 = 100$ sonobuoys randomly scattered over a square kilometer, each with $n_2 = 100$ optical hydrophones distributed over a 100m depth that are multiplexed onto a single fiber, producing an array of 100 fibers that are transmitted back to the processor. Time delays of at least 1 second must be accounted for due to 1.5km propagation across the array and with $10 - 1000$Hz bandwidth at 1Hz resolution, at least $m = 1000$ time delays of each signal will be required, leading to a requirement for $N = n_1 n_2 m = 10^7$ adaptive parameters. Optimal fully adaptive processing based on covariance matrix estimation and inversion leads to a storage requirements (N^2) in excess of Terabytes, and

processing throughput requirements approaching $N^3/T = 10^{21}$ complex multiplications per second, where the re-adaptation time T is assumed to be 1 second. Even fast constrained algorithms that require between $N^2 = 10^{14}$ and $N^3/m^2 = 10^{15}$ operations per sample, yield astronomical processing throughputs approaching 10^{18} operations/second. Since new targets can appear within $1 - 10$s of seconds, and the array can drift to a new configuration requiring re-adaptation in this same time scale, efficient perturbative approaches may not be effective at reducing these required throughputs. This is the reason why DSP approaches utilize suboptimal computationally efficient processing schemes, such as sub-array adaptation, single stave processing, or transform immediately to the frequency domain. These techniques decreases the generality, flexibility, and optimality of the resulting adaptive systems. For example, reducing the number of adaptive parameters limits the ability to null large numbers of interfering sources, or to accommodate nearfield or wave-guided acoustic fields. We instead utilize all optical processing of the optical signals produced by the hydro-phone arrays in order to implement fully adaptive multi-octave sonar array processing.

2 Hydro-phone Sensor Interface

Time-multiplexed fiber-optic hydro-phone arrays consist of a sequentially interrogated array of path length mismatched Mach-Zehnder interferometer illuminated by a laser pulse as shown on the left side of Figure 2.[4] In each interferometer the input pulse is split in two, one arm of which is perturbed by the strain caused by the locally detected sonar signal, and then these two signals are recombined. Optimum interferometric sensitivity for the conversion of the phase modulated signal into an intensity requires appropriate operating point biasing of the interferometer, but

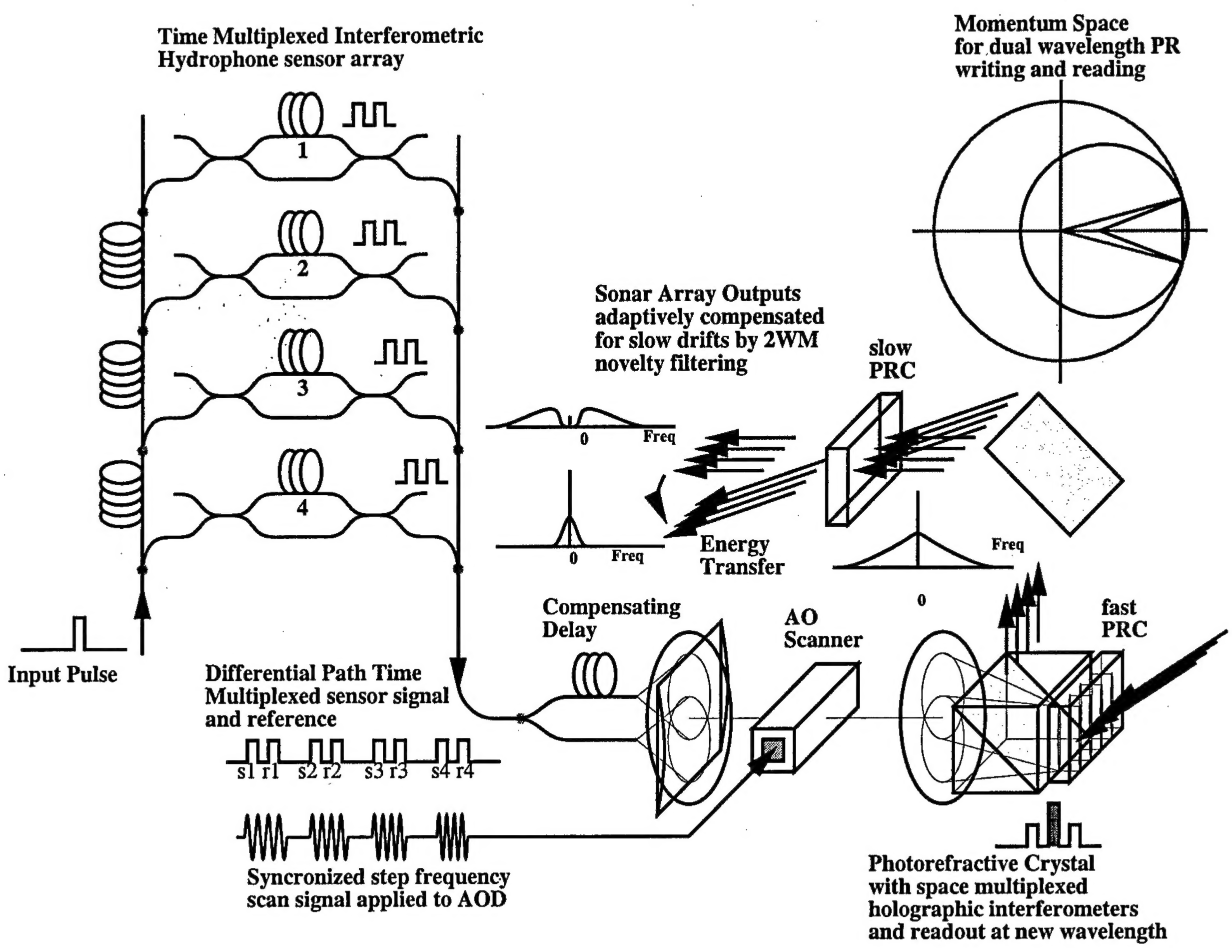

Figure 2: Sensor-Processor Interface: Optical preprocessing of the sonar signal to adaptively compensate for slow hydro-phone drift and novelty filtering of the optical carrier prior to beamforming.

this bias point may drift due to temperature and mechanical fluctuations. However, the fringe locking circuitry should not be placed in the ocean and must be remoted, so the interference is delayed by path length mis-matching the two arms by more than the pulse length, combining even longer time-delayed versions of the dual pulses coming from all the fiber interferometers, propagating back to the receiver, demultiplexing and then re-delaying the pulse pairs from each interferometer by the same delay so the two terms will interfere. Sending both signals down the same fiber avoids phase perturbation sensitivity except where it is desired within the hydro-

phone interferometer. Before beamforming, the time-multiplexed signals from the sequentially addressed hydrophones must be demultiplexed into individual channels, and combined with a phase stabilized interferometer locked at the appropriate bias point. Previously, discrete fiber switches, delays, couplers, detectors, stretchers, and dithering and locking circuitry have been utilized, with duplication of the hardware required for every additional hydro-phone sensor.[5] Figure 2 shows instead an efficient parallel time-multiplexed interferometric architecture used to de-multiplex the signals, compensate for drift in the operating point of the hydro-phone interferometers, and also to filter the unwanted optical carrier and fiber noise prior to injection into an optical beamforming processor. The time-multiplexed hydro-phone signals are split, appropriately delayed in two vertically separated fibers both of which are demultiplexed by the acoustooptic (AO) scanner interferometer that is synchronously driven by a frequency stepped scan waveform. The time-aligned scanned signals are focused back into overlapping spots that write the appropriate spatially multiplexed gratings in a fast photorefractive crystal (PRC). The readout of the rapidly responding photorefractive grating by a counter propagating plane wave produces phase modulated beams carrying the hydro-phone modulation signals as well as the slow modulations due to hydro-phone thermal drift. These modulated signals are coupled with an array of reference beams in a second slower PRC where two wave mixing couples out low frequency modulations due to fiber and hydro-phone drift leaving a spatially multiplexed array of hydro-phone modulated optical signals ready for beamforming. This system implements all the functions of the fiber-optic hydro-phone sensors but without the parallel discrete array of components required by current implementations. [6]

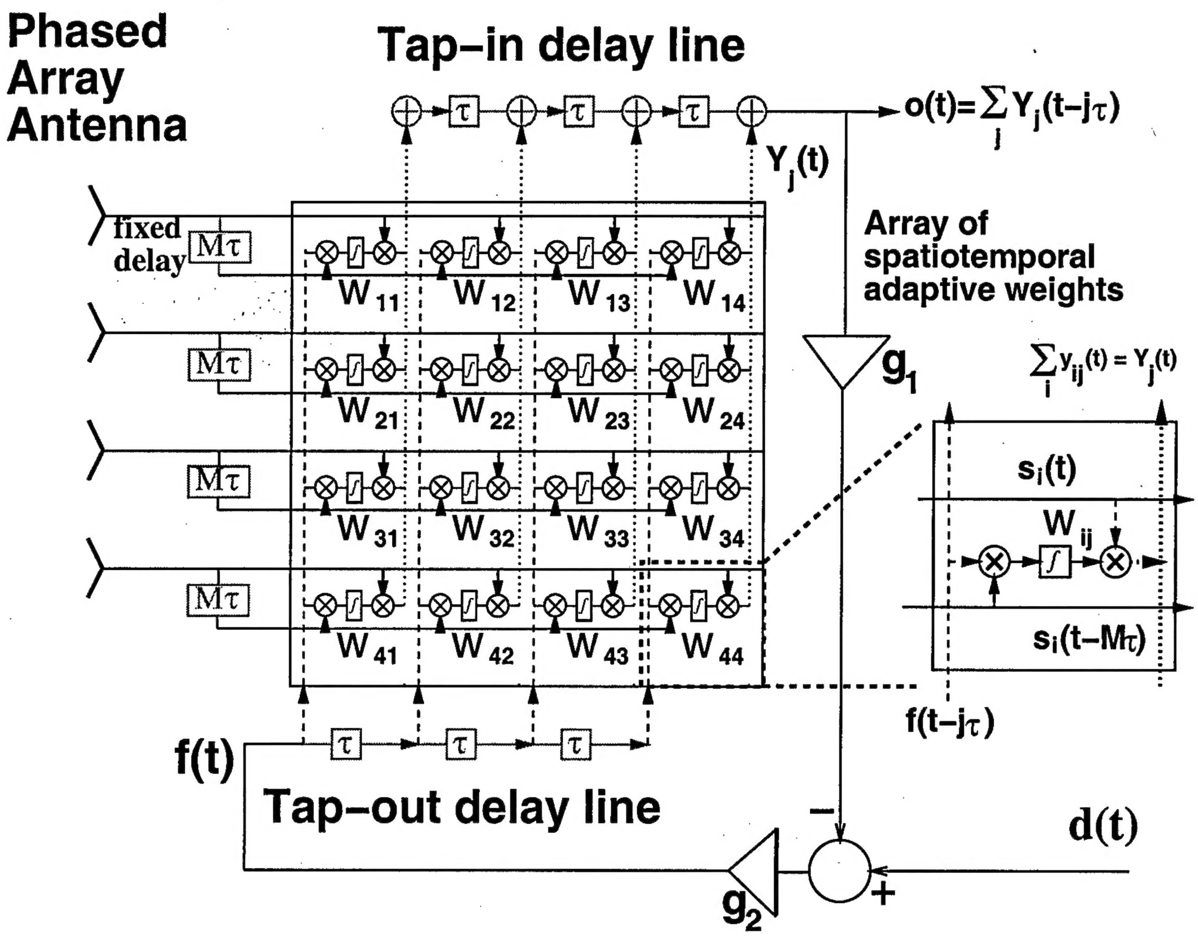

Figure 3: BEAMTAP algorithm for broadband squint-free true-time-delay beamforming using a single output tap-in delay line and a single feedback tapped-delay-line for adaptive calculation of the weights within the array as time integrated correlations. Time delay is not required within the array of weights.

3 Sonar BEAMTAP

The beamforming processors for sonar and RF phased array systems are based on the BEAMTAP algorithm, shown in Fig 3. Each hydro-phone sensor element output $s_i(t)$ is multiplied at each resolved time step by a linear array of weights W_{ij} located along a given row of the weight matrix. Each product is then summed along the column with the corresponding products from the other array elements. The resulting sum is fed into a scrolling delay line which continuously

accumulates its inputs giving an overall output

$$o(t) = \sum_j^M \int \delta(t' - [t - j\tau]) \sum_i^N W_{ij} s_i(t) dt' = \sum_j^M \sum_i^N s_i(t - j\tau) W_{ij}^*, \tag{1}$$

where N is the number of antenna elements and M is the total number of taps. The weights in BEAMTAP are calculated using conventional LMS adaptation [7, 8] but with a reference signal applied to a tap-out delay line as shown. These weights are implemented as holographic gratings in a photorefractive crystal (PRC) volume, and each resolvable hologram acts as an interferometric time integrating multiplier in the form

$$W_{ij}^*(t) = \int_{-\infty}^{t} s_i^*(t_1) f(t_1 + (j - M - 1)\tau) dt_1. \tag{2}$$

Hence, the resulting LMS output is

$$\begin{aligned} o(t) &= \sum_j \sum_i \int \delta(t' - [t - j\tau]) s_i(t') \int_{-\infty}^{t'} s_i^*(t_1) f(t_1 + (j - (M-1))\tau) dt_1 dt' \\ &= \sum_j \sum_i s_i(t - j\tau) \int_{-\infty}^{t} s_i^*(t_2 - j\tau) f(t_2 - (M-1)\tau) dt_2. \end{aligned} \tag{3}$$

This algorithm is nearly equivalent to the conventional time-delay-beam-forming (TDBF)[7, 8] except for the simple time shift $T = (M-1)\tau$ in the reference signal $f(t)$ which implies anticipation of the output $o(t)$. This apparent causality problem can be overcome by delaying a copy of the antenna signals $s_i(t)$ by T and using the delayed version to write the weights while the undelayed version is used for beamforming. The number of tapped-delay-lines in this case has been dramatically reduced from N as required by the conventional TBDF to just 2. In BEAMTAP, this approach enables the processing of very large arrays with thousands of receiving elements each with multi-octave bandwidths using only 2 tapped-delay-lines, and it is especially well suited to optical implementation [2]. For the sonar scenario, the tap-out delay line would be implemented with a liquid-crystal-on-silicon scrolling spatial light modulator (LCOS

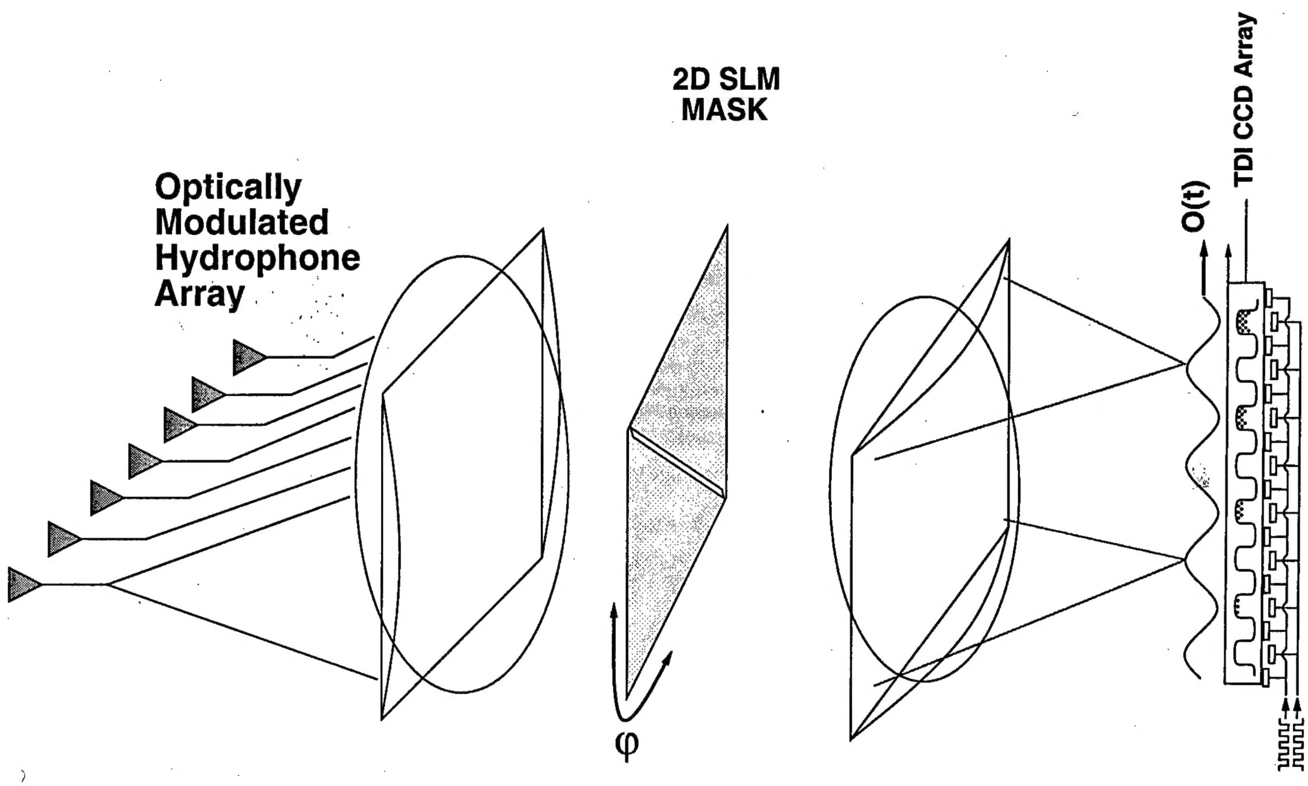

Figure 4: Simplified implementation of the optical sonar BEAMTAP system that forms a main beam of the receptivity pattern in the direction of the angular orientation of the slit. Other main beam orientations are obtained by mechanically rotating the slit.

SLM) while a time-delay-and-integrate charge coupled device (TDI CCD) is used for the tap-in delay line.[9] The adaptive weights can be implemented with an optically addressable SLM or a photorefractive crystal.

The simplest implementation of true-time-delay beamforming based on this approach utilizes an optical matrix-vector multiplier architecture[10] shown in Fig. 4, where a slit is used as the non-adaptive weight matrix. In contrast to the adaptive system, this system only works for a linear equi-spaced array, although similar architectures could be used for other regular tesselations such as circular arrays. To detect a broadband signal from a given look angle, the slit is rotated to the appropriate angle to compensate for the hydro-phone array delays and the transmitted

light is imaged and interferometrically detected on a scrolling TDI CCD detector which sums the modulated spatio-temporal field to yield the desired beamformed output.

For adaptive sonar array processing of a passive environment using a linear array, where the desired signal may not be known a priori but its bandwidth and desired look directions are specified, we can use the P-vector LMS algorithm.[11] Consider the architecture in Fig. 5 for processing linear sonar arrays and simultaneously forming many adaptive beams in a continuous fan covering the entire space of observable angles. After pre-processing, each hydro phone launches an optical field through a PRC and onto a hyperboloid mirror with 45^0 facets whose tilt angles determine the look angles of the array just as in the slit angle case in Fig. 4. Incident sonar signals corresponding to any of these predetermined look directions will be reflected onto a second 2-dimensional TDI CCD where they will be appropriately delayed to synchronize their timing and summed to achieve coherent array gain each respective direction, and these signals are fed back as steering signals for the array. Any subsequent Bragg matched incident energy will be diffracted towards the scrolling output detector where it is interferometrically detected and time integrated in a moving coordinate frame. In this mode, each photogenerated carrier is accumulated and shifted along at a constant velocity resulting in a de-skewed reconstruction of the incident sonar signal. Now suppose a jammer signal or interfering source (for example, a propeller) switches on at some later time. It will not reflect off the hyperbolic mirror with the correct phase factor to match the CCD shift rate and achieve full array gain, but because it could be substantially larger than the sonar signal of interest, it may still dominate the CCD output. This CCD output signal is fed back into the scrolling SLM which interferes with the modulated optical field from the hydro-phone array to write a grating in the PRC. Dynamic gratings will build up for the look direction from which jamming sonar signals are incident due

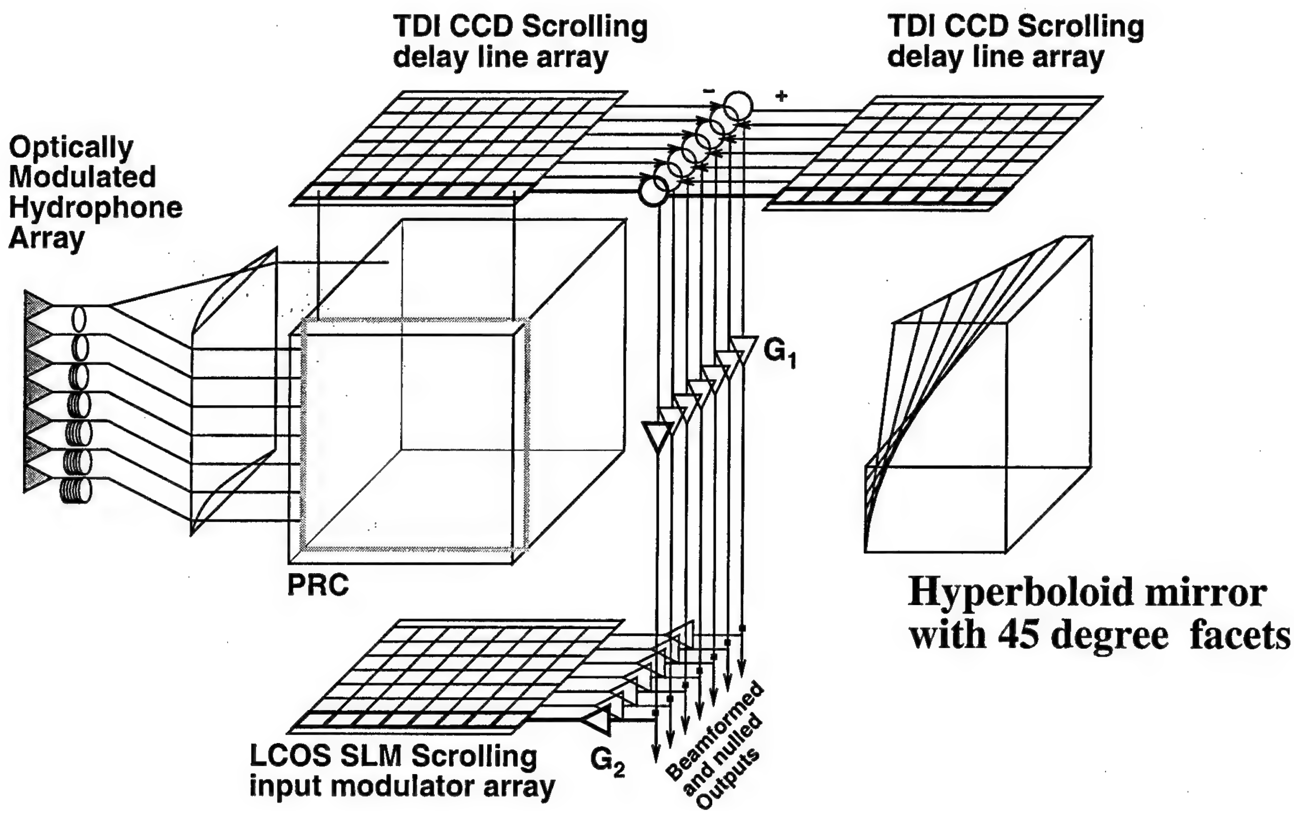

Figure 5: Optical implementation of a multi-channel P-vector beamforming and nulling system for sonar signals. The tilt of the slices of the hyperboloid mirror determines the desired look angle of the phased sonar array.

to the correlations of these signals with their leakage through the sidelobes of the beam-steered array function. The adaptive loop adjusts the grating amplitude to null unwanted interference sources at the electronic difference nodes. This system is capable of simultaneously forming multiple beams, each independently nulled.

Key to either of these implementation is the use of a CCD array in TDI mode. A linear CCD array can be operated in this mode by opening the transfer gate during the CCD readout clocking interval. Under normal operation, charge builds up on the photo sites proportional

to the incident light intensity while at the same time these sites are isolated from the CCD shift registers by a voltage barrier applied to the transfer gate. The transfer of charge to the CCD shift registers begins by stopping the horizontal shift clocks while removing the potential barrier imposed by the transfer gate to allow the transfer of charge. To operate in TDI mode, the transfer gate is permanently held high so that charge is continuously transferred to the CCD shift registers while they are simultaneously and continuously shifted by their horizontal clocks. Photogenerated charge carriers are accumulated and shifted along at a constant velocity $V_{CCD} = \Delta x \cdot f_s$ by the applied clock signal. In this way, the CCD acts as a sampling detector linearly moving at velocity V_{CCD}.

4 Demonstration of TTD with TDI CCD

A key component of the optical processor is the the tap-in delay line implemented with a TDI CCD. The detection technique of using a linear CCD array operating in TDI mode to implement BEAMTAP's scrolling tap-in delay line was experimentally investigated and demonstrated. Figure 6 shows an experimental setup to demonstrate the true-time-delay capability of a TDI CCD necessary for squint-free sonar beamforming. A laser beam is focused into an acousto-optic modulator (AOM) and the diffracted beam is collimated by L_2 as shown. The collimated beam is then focused to a diffraction limited spot only a few pixels in width on a CCD array.

The AOM is then modulated with a narrow pulse train mixed with an RF carrier. The temporal width of the pulse is chosen to be no more than a few pixel clock intervals while the pulse repetition interval (PRI) of the train was made longer than the time required to collect the entire CCD line (inverse line rate) so that only a single pulse fit in the entire CCD line acquisition

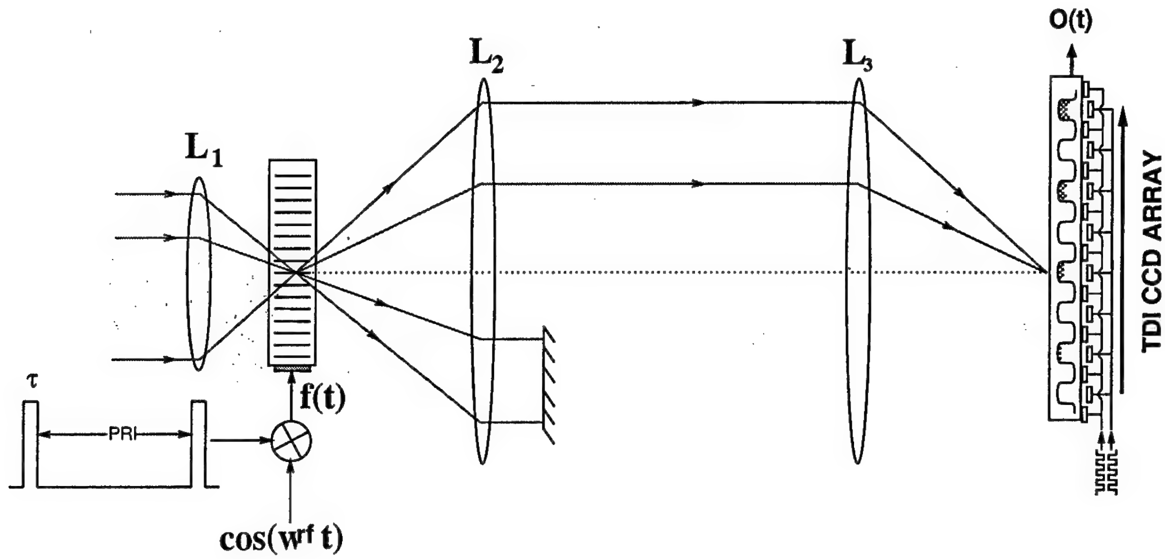

Figure 6: A modulated square pulse of duration τ is used to drive an AOM. The diffracted beam from the AOM is focused onto a TDI CCD while the DC beam is blocked by a spatial filter. The effect is for the CCD to sample the modulated beam resulting in a recovery of the modulating pulse train. Different positions on the array correspond to different time delays of the sampled pulse in the temporal output $o(t)$.

window. With this setup the CCD acts a sampler reproducing the pulse at a given pixel location. When the focused spot is moved to another location on the CCD array, the pulse is reproduced as before but this time at a different temporal location relative to the first pulse. Hence, different pixel locations on the CCD array correspond to a tapped scrolling true-time-delay line as desired.

Figure 7 shows the experimental results for illumination at various points on the CCD array. The results were obtained for a pixel clocking rate of 23KHz and a PRI of 90 ms. The same pulse is reproduced without distortion at all other locations on the CCD demonstrating true-time-delay such that all the temporal frequency components in the pulse are delayed by the same amount. At this pixel rate and with 2048 pixels on the array, the maximum time delay available is about 85-ms, and this can be increased to nearly 1 second by slowing down the CCD shift clocks.

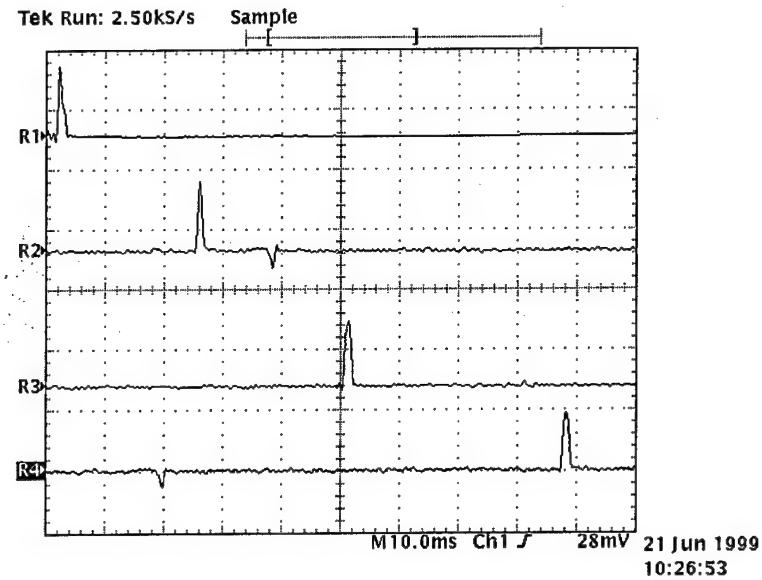

Figure 7: Experimental results showing TTD as the pulse is moved to different positions on the CCD array.

5 System Simulations

A simulation of the BEAMTAP algorithm with jammer nulling is illustrated in Fig. 10. In this example the input consist of a chirp signal and a broadband jammer. Figure 8 shows the spatio-temporal Fourier space of a simulated input sonar signal and jammer used in a simulation of the optical beamformer and nuller. The desired signal is a nearfield broadband Gaussian chirp with bandwidth 1.1 KHz to 1.9 KHz apodized by a Gaussian window. The jammer is a broadband filtered Gaussian white noise signal spanning 0.5 KHz to 2.5 KHz with angle of arrival of 0.2 radians. The matrix in the far left of Fig. 10 illustrates the spatio-temporal sequence of the input array signals, linear chirp plus jammers. The matrix on the right represents the weights of the adaptive array after 1.02s of adaptation. 64 antenna elements and 64 time delays on each

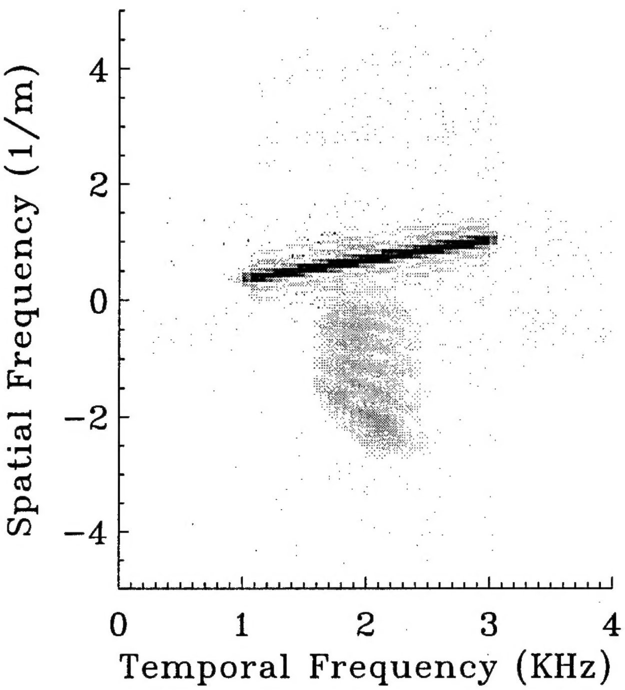

Figure 8: Fourier space of simulated input signal detected by a linear array of 64 sonar hydrophones, showing a strong far-field interference source and a near-field desired signal.

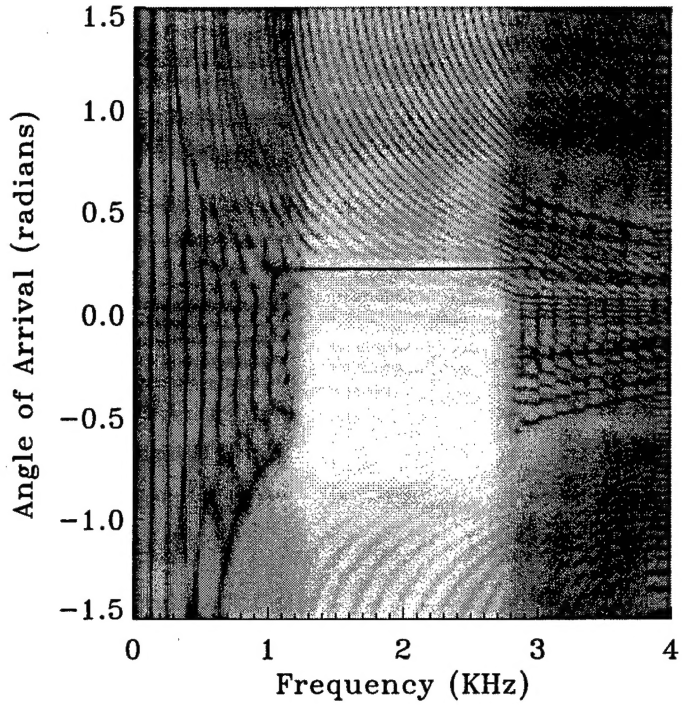

Figure 9: Receptivity pattern that demonstrates true-time-delay sonar array beamforming towards the near-field signal and squint-free near-field interference nulling.

delay line were used on this simulation, providing us with an array of 64×64 adaptive weights. Notice that the time and phase delays caused by the curved wavefronts of the near-field signal are exactly compensated for by the diffraction off of the curved grating slice in the PRC in a fully adaptive fashion. Similar gratings would compensate for delays associated with arbitrary array configuration such as a conformal or flexible arrays on the hull of a submarine or along the sea floor, towed or floating hydro-phone arrays in a turbulent sea environment, or additional delays or phases from the fiber feed network. The thin slice below the weights represents the

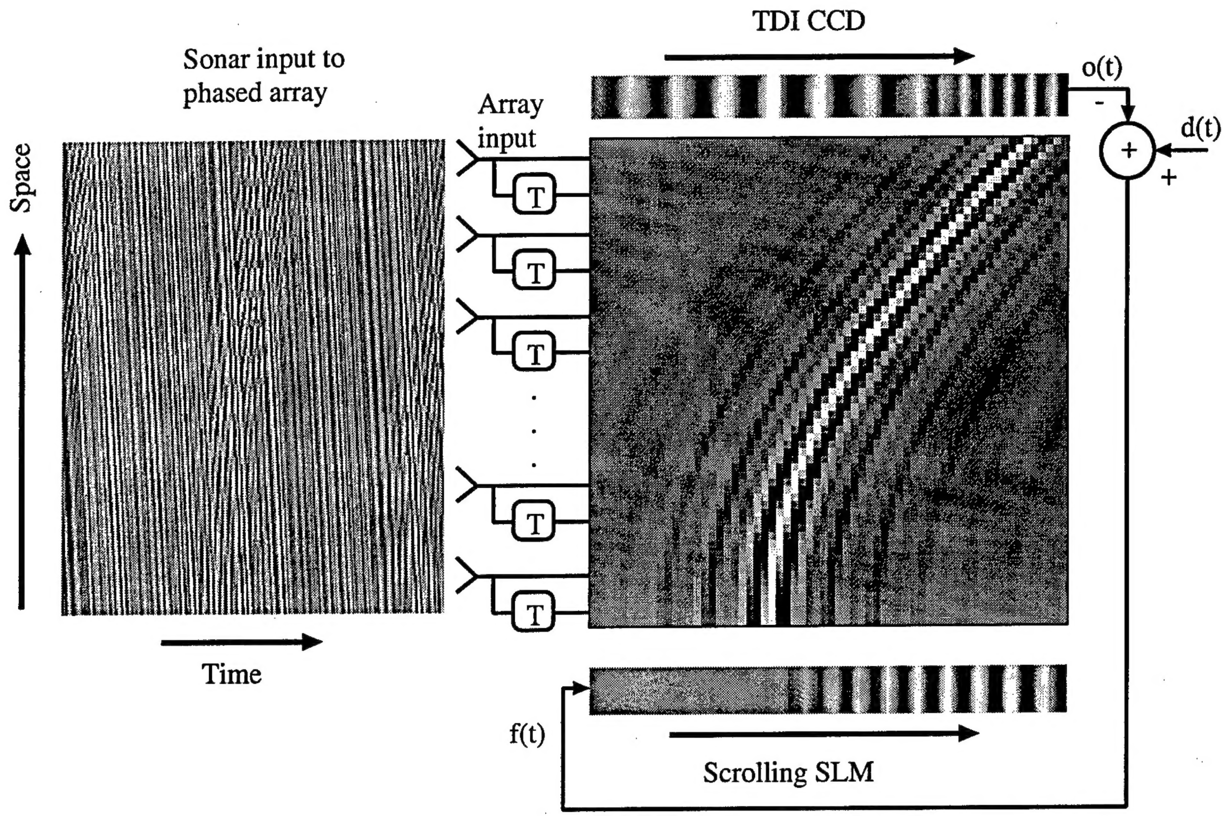

Figure 10: Simulation of BEAMTAP algorithm in the presence of a near-field chirp signal and two jammers. The arriving signal history on each of the 64 hydro-phone array elements is shown on the left, and the BEAMTAP processor signals on the right. The curved peak in the weight matrix compensates for the near-field geometry of the desired chirp signal, and its profile implements an FIR bandpass filter matched to the chirp bandwidth.

modulation of the scrolling SLM which implements the tap-out delay line. The thin slice above the weights represent the accumulating output in the TDI CCD, the tap-in delay line. Notice in Fig. 9, the strong response of the receptivity pattern in the directions of the desired near-field signal over the input signal bandwidth, the narrow squint-free null towards the broadband jammer (0.2 radians) over its entire bandwidth consistent with true-time-delay processing.

Figure 11 shows a sample of delayed input chirps incident on individual hydrophones and

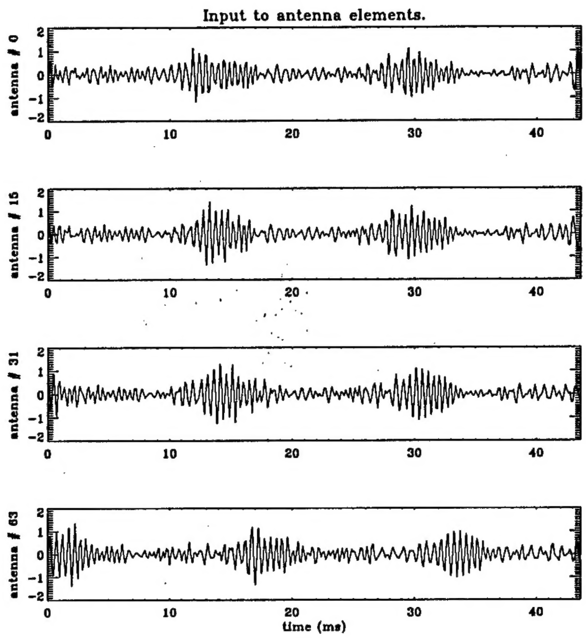

Figure 11: Chirp inputs to each individual hydro phone buried in noise.

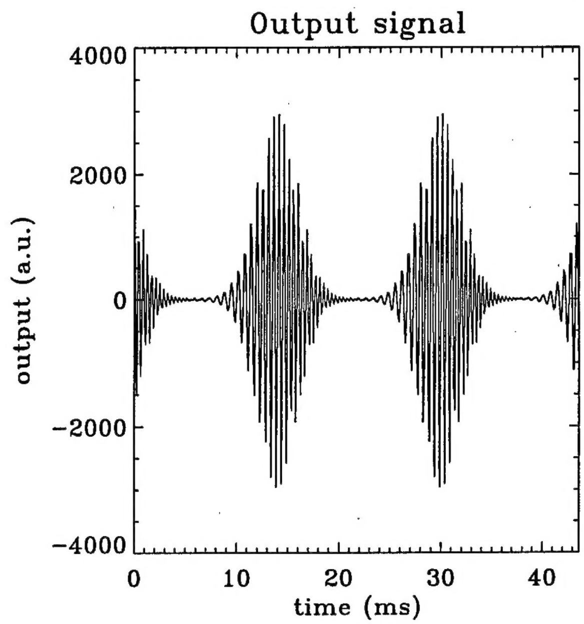

Figure 12: Cohered output from the array showing TTD processing achieving the full array gain on large fractional bandwidth signals

buried in noise. The broadband true-time-delay and coherent summation of each hydro-phone contribution is clearly demonstrated by the output in Fig. 12 which demonstrated the full array gain. The system is capable of performing TTD beamforming necessary to avoid beam squint over the frequency range of the chirp.

6 Conclusions

We have presented novel architectures for true-time-delay sonar beamforming and jammer excision that exploit the optical nature of the data from hydro-phone sonar arrays to implement real-time adaptive processing. The capability of generating TTD processing using a CCD operating in TDI mode was also demonstrated. Simulations have been carried out to demonstrate

the true-time-delay capability of these processors as well as the practical considerations for implementation of these architectures.

We wish to acknowledge the support of Dr. John Lee of NRL through grant no. N00014-97-C-2039 and N00014-96-C-2045.

References

[1] K. Wagner, S. Kraut, L.Griffiths, S. Weaver, R. Weverka, and A. Sarto, "Efficient true-time-delay adaptive array processing," in *Proc. SPIE, vol. 2845,*, 1996.

[2] G. Kriehn, A. Kiruluta, P. E. X. Silveira, S. Weaver, S. Kraut, K. Wagner, T. Werveka, and L. Griffiths, "Optical beamtap beamforming and jammer nulling system for phased array antennas," *Submitted to Applied Optics* , 1991.

[3] A. Kersey, "Demonstration of a hybrid time/wavelength division multiplexed interferometric fiber sensor array," *Electronics Letters* **27**(7), pp. 554–555, 1991.

[4] A. Kersey, A. Dandridge, and A. Tveten, "Time-division multiplexing of interferometric fiber sensors using passive phase-generated carrier interrogation," *Optics Letters* **12**(10), pp. 775–777, 1987.

[5] A. Kersey, K. Dorsey, and A. Dandridge, "Demonstration of an 8-element time-division multiplexed interferometric fiber sensor array," *Electronics Letters* **24**(11), pp. 689–691, 1988.

[6] A. Dandridge and G. Cogdell, "Fiber optic sensors for navy applications," *IEEE LCS* , p. 81, 1991.

[7] B. Widrow, P. Mantey, L. Griffiths, and B. Goode, "Adaptive antenna systems," *Proceedings of the IEEE* **55**, p. 2143, 1967.

[8] B. Widrow and S. D. Stearns, *Adaptive Signal Processing*, Prentice-Hall, 1985.

[9] K. Bromley, M. A. Monahan, R. P. Bocker, A. C. Louie, and R. D. Martin, "Incoherent optical signal processing using charge-coupled devices (ccds)," in *Photo-Optical Instr. Eng.*, vol. 118, IEEE, 1977.

[10] J. Goodman, A. R. Dias, and L. Woody, "Fully parallel, high speed incoherent optical method for performing discrete fourier transforms," *Optics Letters* **2**, 1978.

[11] L. J. Griffiths, "A simple adaptive algorithm for real-time processing in antenna arrays," *Proceedings of the IEEE* **57**(10), p. 1696, 1969.